

Unveiling the Human-like Similarities of Automatic Facial Expression Recognition: An Empirical Exploration through Explainable AI

F. Xavier Gaya-Morey^{1,2,3†}, Silvia Ramis-Guarinos^{1,2,3†},
Cristina Manresa-Yee^{1,2,3*†}, José M. Buades-Rubio^{1,2,3†}

¹Group of Computer Graphics, Computer Vision and AI (UGIVIA),
Universitat de les Illes Balears (UIB), Carretera de Valldemossa, km 7.5,
Palma, 07122, Illes Balears, Spain.

²Research Institute of Health Sciences (IUNICS), Universitat de les Illes
Balears (UIB), Carretera de Valldemossa, km 7.5, Palma, 07122, Illes
Balears, Spain.

³Department of Mathematics and Computer Science, Universitat de les
Illes Balears (UIB), Carretera de Valldemossa, km 7.5, Palma, 07122,
Illes Balears, Spain.

*Corresponding author(s). E-mail(s): cristina.manresa@uib.es;
Contributing authors: francesc-xavier.gaya@uib.es; silvia.ramis@uib.es;
josemaria.buades@uib.es;

†These authors contributed equally to this work.

Abstract

Facial expression recognition is vital for human behavior analysis, and deep learning has enabled models that can outperform humans. However, it is unclear how closely they mimic human processing. This study aims to explore the similarity between deep neural networks and human perception by comparing twelve different networks, including both general object classifiers and FER-specific models. We employ an innovative global explainable AI method to generate heatmaps, revealing crucial facial regions for the twelve networks trained on six facial expressions. We assess these results both quantitatively and qualitatively, comparing them to ground truth masks based on Friesen and Ekman's description and among them. We use Intersection over Union (IoU) and normalized correlation coefficients for comparisons. We generate 72 heatmaps to highlight critical regions for each expression and architecture. Qualitatively, models with pre-trained weights

show more similarity in heatmaps compared to those without pre-training. Specifically, eye and nose areas influence certain facial expressions, while the mouth is consistently important across all models and expressions. Quantitatively, we find low average IoU values (avg. 0.2702) across all expressions and architectures. The best-performing architecture averages 0.3269, while the worst-performing one averages 0.2066. Dendrograms, built with the normalized correlation coefficient, reveal two main clusters for most expressions: models with pre-training and models without pre-training. Findings suggest limited alignment between human and AI facial expression recognition, with network architectures influencing the similarity, as similar architectures prioritize similar facial regions.

Keywords: explainable Artificial Intelligence, facial expression recognition, human-like, cognitive anthropomorphism, deep learning, empirical evaluation

1 Introduction

Facial expressions are a rich and salient source of information for human communication. While facial expressions are not emotions themselves, they serve as a visual representation of an individual’s emotional state as they offer observable cues that can convey emotions effectively. Their universality has been a topic of debate [1]: some argue that certain facial expressions may vary across cultures or contexts, suggesting that their interpretation may not be entirely universal. However, a significant body of research builds upon the work of Ekman, who identified six fundamental and universally recognized facial expressions: anger, happiness, surprise, disgust, sadness, and fear [2]. This set of facial expressions do not convey the wide range of different expressions humans can do, but they have been the basis for understanding and interpreting emotional states in research.

Research on automatic Facial Expression Recognition (FER) is a very active field due to its practical application in areas such as medical diagnosis and treatment [3], human behavior analysis [4, 5], or human-computer interaction [6, 7]. The development of FER systems has been a topic of interest for computer vision experts, who have looked to human vision research for insights into the visual perception process. In the early stages of FER research, emphasis was placed on extracting facial features or analyzing facial appearance [8, 9]. However, in recent years, significant progress has been made by leveraging deep learning techniques [10, 11].

Deep learning approaches, such as Convolutional Neural Networks (CNNs), have shown remarkable results in FER tasks and achieved state-of-the-art performance. Regarding these systems, humans often exhibit cognitive anthropomorphism [12], wherein they tend to project human-like qualities and expectations onto AI systems, assuming that AI possesses similar characteristics to human intelligence. However, it is important to note that while a deep learning approach may yield high accuracy in recognizing facial expressions, it does not necessarily imply that the underlying decision-making process resembles that of humans [12, 13]. Therefore, studies have started investigating similarities between deep learning approaches and human vision [14, 15], but thorough comparisons of human and AI behavior are still relatively rare.

Mueller [12] examined known properties of human classification (e.g. representation, processing), in comparison with image classifier systems and described design strategies to cope with the differences: change the AI, change the human (e.g. instructing and training humans' expectations) or change the interaction between human and AI (e.g. showing explanations). In the case of changing the AI, mimicking human behavior may help avoiding errors and inconsistencies in performance when compared with humans and improve the deep networks by incorporating critical information for recognition [16, 17].

In the case of human perception, the Facial Action Coding System (FACS) [18] describes anatomically all visually discernible facial movement by defining Action Units (AUs), which are the actions of individual muscles or groups of muscles. Observing and coding a selection of AUs, EMotion FACS (EMFACS), humans can identify prototypical facial expressions that have been found to suggest certain emotions. Mining the literature, we find deep learning models trained with salient regions for human vision [19] or AUs [20, 21] which achieve similar results as human coders with frontal faces and controlled conditions, but the accuracy decreases to below 83% when conditions are not constrained [22].

In this particular study, the focus lies on deep networks trained with facial expression images, primarily because these networks exhibit the ability to handle the challenging conditions of recognition in *in the wild* scenarios [10]. Furthermore, the study specifically deals with still images, rather than dynamic sequences or videos. We seek to answer whether deep networks observe facial AUs regions as defined in EMFACS and how human-like, in terms of visual perception of physical cues, is their processing.

To gain a deeper understanding of the inner workings of deep learning techniques, the integration of eXplainable Artificial Intelligence (XAI) techniques has emerged as a valuable approach [23, 24]. XAI techniques aim to provide explanations on how deep learning models make decisions and generate outputs, enabling human users to comprehend and interpret the results effectively [25]. By applying XAI techniques, we will analyze the human-like perception of deep learning models and explore their similarities with the FACS.

The aim of this work is twofold. On the one hand, we investigate on the similarities of deep networks with facial AUs using explainability techniques to assess how human-like are the deep networks regarding visual perceivable features. On the other hand, we compare different CNNs to study whether they focus on the same regions. Comparisons among the 12 CNNs would clarify whether FER relies on specific zones or on the architecture of the network.

2 FER comparison between human perception and deep learning techniques

There is a scarce number of works comparing thoroughly human perception and deep learning techniques regarding FER. Mining the literature, we find works focused on applying XAI techniques to the FER domain [26–31], but it is out of their scope to explore in depth the similarities or differences regarding the human perception.

Regarding works related to analyzing how human-like are the learned features of deep learning techniques when not trained specifically with them (e.g. using AUs to train the model), Khorrami et al. [32] already considered whether the neural networks learned facial AUs in FER. They proposed an approach to interpret which portions of the face influenced the CNN’s predictions and applied it to the extended Cohn-Kanade (CK+) dataset [33] and the Toronto Face Dataset (TFD) [34]. They visualized the spatial patterns that maximally excite different filters in the convolutional layers of the network (10 selected filters in the conv3 layer). Then, they compared if the facial observed AUs aligned with facial movements by using the KL divergence on the FAU labels given in the CK+ dataset. Their results showed that CNNs are able to model high-level features that correspond to facial AUs.

Prajod et al. [35] also related the automatic FER with AUs. They presented a study on the effects of transfer learning for automatic FER from emotions to pain using the VGG16 architecture and two datasets: AffectNet for emotions and UNBC-McMaster for pain [36]. They applied Layer-wise Relevance Propagation (LRP) saliency maps to visually compare and understand the most influent regions for the classification, both for emotion recognition and for pain recognition, and map those regions with AUs. The results showed that specific AUs related to the facial expressions of contempt and surprise were not relevant for pain recognition.

Deramgozin et al. [37] presented a hybrid framework composed of a main functional pipeline with a CNN to classify input images and an explainable pipeline including a LIME visualization part. It also included a facial AUs extraction part to identify the AUs and a Multi-Layer Perceptron (MLP) classifier which reused the results of the facial AU extractor to reinforce the results obtained by the main functional pipeline. The 13 AUs used in this work were: AU01, AU02, AU05, AU06, AU07, AU09, AU12, AU15, AU17, AU20, AU23 and AU26. They evaluated their CNN and the FAU+MLP system with the CK+ dataset, and they did a visual comparison of the LIME and AUS extracted. The AUs extracted were consistent with Ekman’s basic facial expressions, although they found some differences due to the dataset and the compound emotional categories.

Gund et al. [38] analyzed superficially how different spatial regions and landmark points changed in position over time. They classified expressions using two convolutional networks trained with the CK+ dataset and tested with the SAMM dataset [39]. They highlighted the regions of interest with Class Activation Maps (CAM) and visually compared the AUs of each emotion with the CAM for landmarks for some images.

Zhou et al. [40] did not use XAI techniques, but they found that the pretrained VGG-Face, could spontaneously generate expression-selective units. The accuracy of the system was far lower than humans, but it exhibited hallmarks of human expression recognition (e.g., facial expression confusion and categorical perception). However, the expression-selective units did not exhibit reliable human-like characteristics of facial expression perception.

None of the works reviewed carry out an in-depth comparison between the learning of the model and visually perceptible features observed by humans. Since there are insights both indicating the similarity and the differences between the model learning

and the human perception, in this work we will carry out a thorough quantitative comparison and a qualitative exploration.

3 Facial Expression Recognition

3.1 Datasets

We list four standard datasets widely used in facial expression studies: the Extended Cohn-Kanade (CK+) dataset [33], the BU-4DFE dataset [41], the JAFFE dataset [42] and the WSEFEP dataset [43]. In addition, we include the FEGA dataset introduced in [44]. Some samples from the different datasets can be observed in Figure 1.

The Extended Cohn-Kanade (CK+) dataset [33] contains 593 facial expression sequences from 123 subjects ranging from 18 to 30 years old. These sequences are labelled with one of the 7 emotions (anger, contempt, disgust, fear, happiness, sadness, and surprise) based on the expression of each subject.

The BU-4DFE dataset [41] contains 606 3D facial expression sequences from 101 subjects (58 females and 43 males). Each subject performed six sequences, one for each facial expression (anger, disgust, fear, happiness, sadness and surprise).

The JAFFE [42] dataset contains 213 images from 10 female Japanese actresses posing six basic facial expressions (happiness, surprise, fear, sadness, anger, disgust) and the neutral facial expression.

The WSEFEP [43] dataset contains 210 high-quality images of 30 subjects (14 men and 16 women) posing the six basic facial expression plus the neutral face.

Finally, the Facial Expression, Gender and Age (FEGA) dataset [44] contains 51 subjects (21 females and 30 males) ranging from 21 to 66 years old. Each subject posed six basic facial expressions plus the neutral face. Each subject was also labelled with the age and gender.

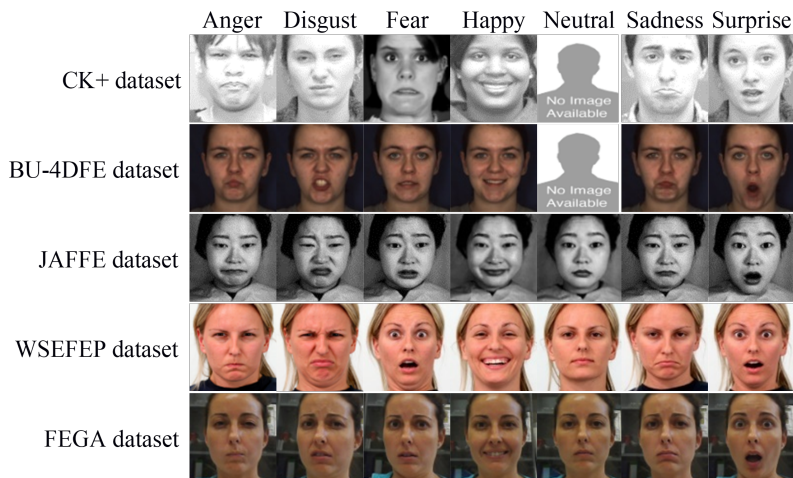


Fig. 1: Samples for each class (by columns) available from each of the datasets (by rows) used in this study.

3.2 Pre-processing and data augmentation

To prepare the input of the datasets used for the training, we need to homogenize the images regarding resolution, color space and face alignment [44]. On the one hand, when training and testing, we prepare the images applying these three steps:

1. Detect the face on the image using the method proposed by Lisani et al. [45].
2. Align the face using the 68 facial landmarks proposed by Kazemi and Sullivan [46] to locate the eyes position and calculate the distance between them. This method was selected for its speed, accuracy and robustness. Further, it is a very well-known technique [47]. We get the angle to rotate the image by drawing a straight line between the eyes, and then, we crop the aligned face.
3. Convert the image to gray-scale and resize it to fit the input of the CNN.

On the other hand, when training, we also augment the number of images applying these two steps:

1. Add variations in terms of lighting. We use the gamma correction technique [48].
2. Add variations in terms of appearance, which aim to cover for small errors in the position of the eyes during the eyes' location detection. The variations are: translation (in both axes), crop (always preserving the eyes, nose and mouth), and mirroring.

3.3 CNN Architecture

We built twelve models used in the literature to classify Ekman's six basic facial expressions: nine well-known models widely used in the computer vision and neuroscience literature (AlexNet [49], VGG16 [50], VGG19 [50], ResNet50 [51], ResNet101V2 [51], InceptionV3 [52], Xception [53], MobileNetV3 [54], and EfficientNetV2 [55]) and three models built specifically for FER (Ramis et al. [44], Song et al. [56] and Wei et al. [57]). We name these three works as SilNet, SongNet and WeiNet respectively. All these CNNs were trained and tested on the datasets described in subsection 3.1, which were pre-processed and augmented following the steps listed in subsection 3.2.

AlexNet, WeiNet, SongNet, and SilNet exhibit simpler architectures compared to the other models, comprising three to five convolutional layers followed by max-pooling layers, and concluding with varying numbers of dense layers. VGG16 and VGG19 are variants sharing a base architecture, distinguished by their use of compact 3x3 convolutional filters across the network and concluding with three fully connected layers, resulting in a total of 16 and 19 layers, respectively. ResNet50 and ResNet101V2 are part of the residual network family [58], which introduced residual learning through skip connections, facilitating the creation of deeper architectures. While ResNet50 comprises 50 layers, ResNet101V2 integrates optimizations such as bottleneck layers and improved skip connections, totaling 101 layers. InceptionV3 and Xception represent advancements over the original Inception [59], employing Inception modules with multiple parallel convolutional operations. Notably, Xception replaces standard Inception modules with depthwise separable convolutions to capture cross-channel and spatial correlations separately, thereby enhancing efficiency and performance. MobileNet [60] is a family of lightweight neural network architectures designed

for efficient deployment on mobile and edge devices. Characterized by depthwise separable convolutions, MobileNet architectures strike a balance between accuracy and computational efficiency, proving suitable for resource-constrained environments. MobileNetV3 incorporates features like inverted residuals, linear bottlenecks, and squeeze-and-excitation modules to further enhance efficiency and accuracy. EfficientNetV2 represents an improvement over the original EfficientNet [61], which introduced compound scaling for simultaneous optimization of model depth, width, and resolution, resulting in improved performance and efficiency. The second version introduces refinements in scaling factors, potentially enhancing overall model performance with fewer parameters.

Table 1 provides a comprehensive overview of each utilized model. By incorporating these diverse architectures and comparing their performance, we aim to gain valuable insights into the impact of architectural choices on FER tasks.

Table 1: Networks used in this study to classify facial expressions. The number of parameters shown corresponds to the obtained model after replacing the final fully-connected layers.

Ref.	Model	Image Size	Pre-training	Parameters
[49]	AlexNet	224x224	No	88.7 M
[57]	WeiNet	64x64	No	1.7 M
[56]	SongNet	224x224	No	172.7 K
[44]	SilNet	150x150	No	184.9 M
[50]	VGG16	224x224	Yes	14.7 M
[50]	VGG19	224x224	Yes	20 M
[51]	ResNet50	224x224	Yes	23.6 M
[51]	ResNet101V2	224x224	Yes	42.6 M
[52]	InceptionV3	224x224	Yes	21.8 M
[53]	Xception	224x224	Yes	20.9 M
[54]	MobileNetV3	224x224	Yes	3 M
[55]	EfficientNetV2	224x224	Yes	5.9 M

The following models utilized pre-trained weights from the ImageNet dataset: VGG16, VGG19, ResNet50, ResNet101V2, InceptionV3, Xception, MobileNetV3, and EfficientNetV2. For these models, we removed the final fully connected layers and replaced them with an average 2D pooling layer and a new fully connected layer, tailored to accommodate the specific number of facial expression classes (anger, fear, disgust, sadness, surprise, and happiness) as defined by Ekman and Friesen [18]. Conversely, the models AlexNet, WeiNet, SongNet, and SilNet were trained from scratch exclusively using facial expression images. Notably, WeiNet, SongNet, and SilNet were purpose-built explicitly for the task of facial expression recognition.

The implementation of the models was carried out in Python, leveraging the Keras library. For the models AlexNet, WeiNet, SongNet, and SilNet, we implemented each layer step by step within the Keras framework. The remaining models were readily accessible through the Keras API, complete with their pre-trained weights from the ImageNet dataset.

3.4 Procedure

We performed a k -fold cross validation with $k = 5$ to train the twelve networks on the five datasets defined in subsection 3.1. To do so, we first grouped the images by users for each dataset, and then split in five the users of each dataset randomly, resulting in five partitions, each containing approximately the same amount of images from each sub-dataset. Finally, following the standard k -fold cross validation procedure, we made all five possible combinations combining four of the splits for the training and leaving the remaining one for testing.

Before starting with the cross validation, we conducted preliminary trainings for each network to properly determine the number of epochs for each one. We determined that 10 epochs were enough to train SilNet [44], AlexNet [49] and WeiNet [57], while MobileNetV3 [54] and EfficientNetV2 [55] required 10 epochs, and SongNet [56] required up to 25 to get proper results. The remaining networks (i.e. VGG16, VGG19, ResNet50, ResNet101V2, InceptionV3, and Xception) only needed 2 epochs to get a good performance.

Summing up, a total of 60 trainings were carried out: 5 for each of the 12 networks, using different splits of the datasets.

4 Measuring what do the deep networks learn and metrics for comparison

4.1 Obtaining the explanations

To analyze the similarities of the learned features of the CNNs to human visually perceivable face features used for recognizing facial expressions, we use the Local Interpretable Model-agnostic Explanations (LIME) [62]. Other techniques that offer visual explanations exist (e.g. feature-based, propagation-based methods), each of them with pros and cons [63], but from the broad ecosystem of visual-based XAI methods, we chose LIME as it is one of the most popular model-agnostic ones [64]. LIME can be applied on any classifier and offers locally faithful explanations of the instance being explained. When LIME is applied to images, explanations are the parts of the image that influence more for the classification. For each architecture, the aim is to attain a global heatmap of the face regions used to recognize each facial expression using LIME. Since it is unfeasible to consider each pixel independently for explanation, clustering techniques are usually applied to construct super-pixels grouping similar pixels. For this purpose, we have used SLIC [65] as the segmentation algorithm to compute the super-pixels that will then be explained by LIME.

Given a neural network architecture R_j (where j is one out of the twelve networks described in subsection 3.3), a training k and an image X_i , we obtain a classification c_{ijk} which corresponds to a facial expression (anger, happiness, sadness, disgust, fear or surprise). Applying LIME, we get the image regions of most interest for the network. The outcome results in an image, L_{ijk} , with values in the range $[0, 1]$, where 0 means minimum importance, and 1 means maximum. This image is stored in gray-scale to be used in further steps.

4.2 Standardization of the explanations

As each image is taken from a different point of view or the face proportions among individuals are different, the coordinates of the regions of interest between two images do not coincide (e.g. eyes, mouth, forehead or nose). Therefore, we standardize all images, that is, we process each image with the explanation already computed, to make all regions of interest correspond to the same image coordinates. The standardization transforms the image using 68 landmarks on the original image, using the already mentioned method [46]. We then add border landmarks, 17 on the top border and 4 on each corner of the image, to achieve a total of 89. The standard position of each landmark is shown in Fig. 2. The triangulation is done by applying the Delaunay algorithm and it will be used to transform each image X_i .

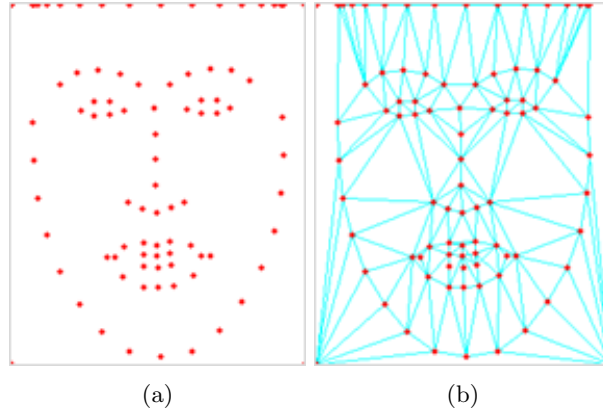


Fig. 2: (a) Standard image with landmarks. (b) Standard image with landmarks and triangulation.

The image L_{ijk} is transformed into S_{ijk} by making the landmarks coincide with the standard position. Being $S_{ijk} = T(L_{ijk}, X_i)$, for each triangle in the standard image, we achieve the coordinates in the image X_i . Then, we calculate the affine transformation considering that the three vertices must coincide, and we apply it to copy the information from image L_{ijk} to S_{ijk} . The whole explanation and normalization process is depicted in Fig. 3, where an example is shown for each expression.

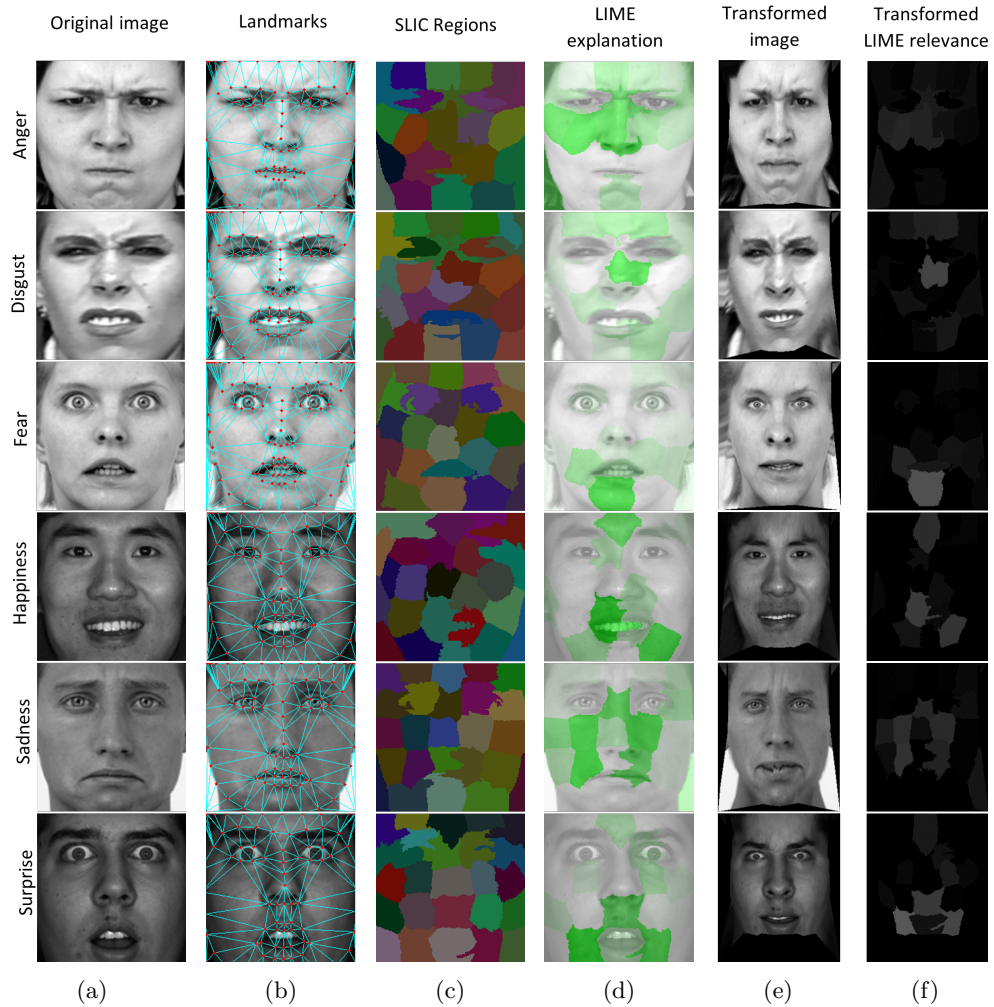


Fig. 3: Images from the different steps involved in the explanation of an image. By rows, an example of each class: Anger, Disgust, Fear, Happiness, Sadness and Surprise. By columns: a) image being explained, b) detected face landmarks, c) super-pixels computed using SLIC segmentation, d) LIME explanation, e) transformed input image using the normalized landmarks coordinates, and f) transformed LIME relevance for each region in gray scale (for further heatmap computation), using the same landmarks.

4.3 Obtaining the importance heatmaps

Once we achieve the LIME transformed images, we can operate with them. Given a coordinate and any LIME transformed image S_x , the coordinate will correspond to

the same face region in all images. Given a network j , a training k , and a set of images A , we can build the heatmap calculating the average of the LIME transformed images (see Eq. 1).

$$H = \frac{\sum_{X_i \in A} S_{ijk}}{\text{card}(A)} = \frac{\sum_{X_i \in A} T(L_{ijk}, X_i)}{\text{card}(A)}, \quad (1)$$

where $\text{card}(A)$ is the cardinal of the set A . We calculate the heatmap for each network, training and facial expression. That is:

A_{jkc} = LIME images built with the network j , training process k and whose classification is c ($c \in \{\text{Anger}, \text{Disgust}, \text{Fear}, \text{Happiness}, \text{Sadness}, \text{Surprise}\}$). We have conducted five trainings for each of the twelve networks, so we can group the explanation images in different ways to make up the heatmaps (see Eq. 2).

$$H_{jkc} = \frac{\sum_{I \in A_{jkc}} I}{\text{card}(A_{jkc})}, H_{jc} = \frac{\sum_{I \in A_{jc}} I}{\text{card}(A_{jc})}, H_c = \frac{\sum_{I \in A_c} I}{\text{card}(A_c)}, \quad (2)$$

where the sum of two images is done pixel-wise. All heatmaps are images with pixel values in the range $[0, 1]$, which indicate the pixel’s probability of being used by the network to classify the image in one of the facial expressions c . Values close to 1 have more influence over the classification of the expression, while values closer to 0 are less important for the classification. H_{jkc} are heatmaps summarizing the explanations of a single training (approximately 100 images per class); H_{jc} group different trainings for the same network, showing which are usually the important regions for a model ($100 \cdot 5 = 500$ images per class); finally, H_c also group the results obtained by different networks, showing which are the most relevant regions globally among all networks ($100 \cdot 5 \cdot 12 = 6000$ images per class).

4.4 Ekman masks construction

We build Ekman masks following the specifications defined by Friesen and Ekman [66], to compare the influential face regions considered by the networks with anatomically visually discernible features related to emotions (i.e. EMFACS). EMFACS defines facial AUs related to facial expressions (see Table 2), and each AU relates to the movement of two or more landmarks. Based on this, we build an AU-landmark related Ekman mask for each facial expression.

To determine the landmarks involved, we use the relations described in Perveen and Mohan’s work [67]. Based on the landmarks, we mark visually the face areas involved in the expression, to obtain an Ekman mask for every expression following Friesen and Ekman’s [66] description (see Fig. 4).

Given a facial expression, to determine the important region, the AUs are taken into account. For a given AU, the corresponding landmark is identified, or alternatively, the triangle of landmarks that includes it. If it matches a landmark, that landmark and its vicinity are marked as an important region. If the AU falls within a triangle (or on an edge), the triangle(s) that include it are marked. Subsequently, the relationship between AUs is evaluated to merge related regions.

Table 2: Facial expressions described by AUs [67].

Facial expression	Facial AUs
Anger	4, 5, 7, 23
Disgust	9, 15
Fear	1, 2, 4, 5, 7, 20, 26
Happiness	6, 12
Sadness	1, 4, 15
Surprise	1, 2, 5, 26

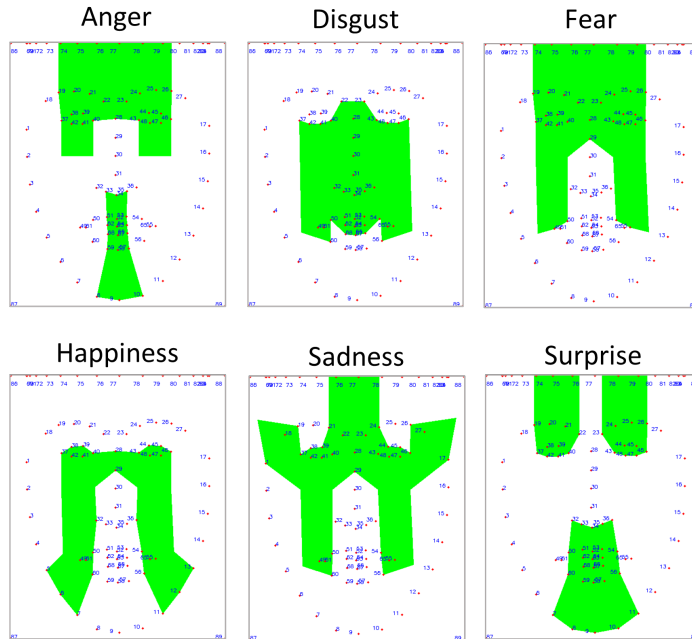


Fig. 4: Face areas involved in each expression, following Friesen and Ekman’s [66] description.

4.5 Metrics for heatmaps and masks comparison

To assess the obtained results and explore the computed heatmaps for the different networks, we use two different metrics: Intersection over Union (IoU) and normalized correlation coefficient.

On the one hand, we use the IoU to assess the difference between two masks, where only binary data is present. This is the case when comparing thresholded heatmaps with the Ekman masks described in subsection 4.4. Considering two binary images I_1 and I_2 of equal dimensions $W \times H$ containing only values in $\{0, 1\}$, then the IoU is computed as in Eq. 3.

$$IoU = \frac{\sum_{x=1}^W \sum_{y=1}^H I_1(x, y) \wedge I_2(x, y)}{\sum_{x=1}^W \sum_{y=1}^H I_1(x, y) \vee I_2(x, y)}. \quad (3)$$

On the other hand, to evaluate how similar are the face regions influencing the classification of facial expressions among network architectures, we use the Normalized Correlation Coefficient, which better addresses the comparison of gray-scale images. Given two heatmaps, $H_1(x, y)$ and $H_2(x, y)$, we calculate the coefficient with Eq. 4.

$$corr = \frac{\langle H_1(x, y), H_2(x, y) \rangle}{\sqrt{\langle H_1(x, y), H_1(x, y) \rangle \langle H_2(x, y), H_2(x, y) \rangle}}, \quad (4)$$

where $\langle a, b \rangle$ denotes the dot product. This metric is 1 when images are identical, and therefore the maximum similarity, and 0 when a heatmap is the inverse of another one. This value is converted to a distance value as $1 - corr$.

4.6 Procedure

Bearing in mind that we have five trainings for twelve networks, we start by taking a sample of 100 positives per class at random, for a total of 600 images, which will be the images to explain. We use the positives (i.e. the class predicted by the model) and not directly images taken from the class being explained because in the case that the model’s prediction and the truth label do not match, we would not be explaining the model’s decision.

To follow up, we segment each image into approximately 30 regions using SLIC [65] and find the importance of each region using LIME, setting the number of samples to 1,000 and the background (or occlusion color) to black. This results in an explanation in the form of a gray-scale image, where brighter colors represent more relevant regions for the class being explained (see subsection 4.1).

The next step is to standardize the gray-scale explanation images obtaining explanations in a normalized space, where the coordinates of the landmarks have a fixed location (see subsection 4.2). With all standardized explanations, we obtain heatmaps at different levels by grouping explanations of the same class, network and training; of the same class and network (joining trainings); or only of the same class (joining trainings and networks), as seen in subsection 4.3.

Finally, we make use of the computed heatmaps in two ways. The first one is to assess the similarity between the heatmaps and the Ekman masks described in subsection 4.4. To do so, it is necessary to first binarize the heatmaps, which we do by using a threshold selected using Otsu’s method [68], and then we calculate the intersection over union. The second one is to analyze the difference among heatmaps of different networks for the same facial expression. For this, we use the normalized correlation coefficient (converted to distance) and construct different dendograms, to visually show which networks bestow importance upon regions in a more similar way.

5 Results

In this section, we present a comprehensive analysis of our experimental findings. Firstly, we provide the cross-validation outcomes for the distinct neural networks employed in the study. Subsequently, we conduct an in-depth qualitative examination of the heatmaps generated by these networks. Additionally, we quantitatively assess the Intersection over Union (IoU) between the heatmaps and the Ekman masks, shedding light on the degree of similarity between the facial expression recognition capabilities of AI models and humans. Finally, we leverage dendrogram construction as an essential tool for exploring the likeness among heatmaps produced by different networks when presented with the same facial expression.

5.1 Cross Validation

To test the performance of each net, we have calculated the average accuracy across cross-validation test sets. The results are shown in Figure 5. As seen, the obtained results for all networks fall within the range of 80% to 84% accuracy, except for ResNet50, which achieved an accuracy of 74%.

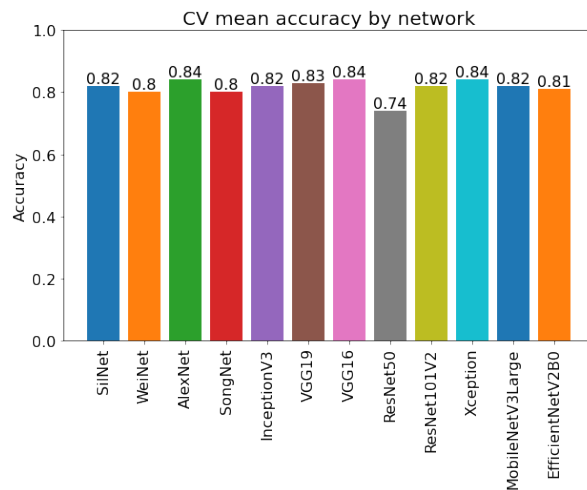


Fig. 5: Mean accuracy of the cross validation for each trained network.

Since the aim of this study is not to maximize these results, we deem the achieved accuracy levels to be satisfactory for proceeding with the subsequent stages of the experiment: an exploration of significant facial regions identified by each network and a comparative analysis with the regions that humans perceive as important.

5.2 Heatmaps

To reflect the importance of the different regions of the face, we have employed the color map shown in Figure 6. The resulting heatmaps of the whole explanation, standardization and summary process described in Section 4 are shown in Figures 7, 8 and 9.



Fig. 6: Color map used to represent the importance of each region in the different heatmaps.

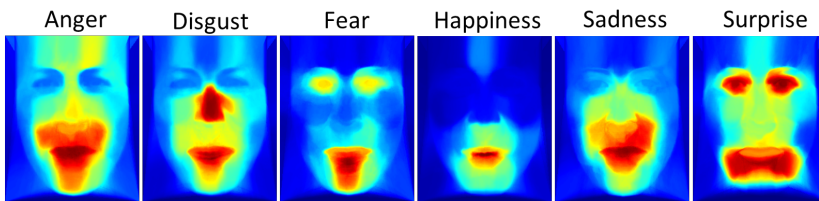


Fig. 7: Resulting per-class heatmaps of the average explanations between all trained networks.

Figure 7 shows the heatmaps summarizing the important regions among all networks for each expression. From these images, we can appreciate the following aspects for the different expressions:

- **Anger:** the relevance is scattered through all the face, with the mouth and surroundings being the most important part. The forehead, nose, cheeks and chin can also be relevant for the models.
- **Disgust:** the nose and mouth are specially relevant for the classification, and so can be the space in between.
- **Fear:** the mouth and the chin are specially important, and the eyes can also be.
- **Happiness:** the most important part is the mouth, although the surrounding regions can also be.
- **Sadness:** the relevance is rather scattered, covering the mouth, nose and the space in between.
- **Surprise:** the important parts are the eyes and the surrounding regions of the mouth.

The mentioned important regions for each facial expression make sense in general comparing with humans' perception: for example, the mouth should be utterly important for the happiness expression (when the person is smiling), the nose should be

important for the disgust expression (wrinkle of the nose), or both the eyes and mouth should be relevant for the surprise expression (they should be wide opened).

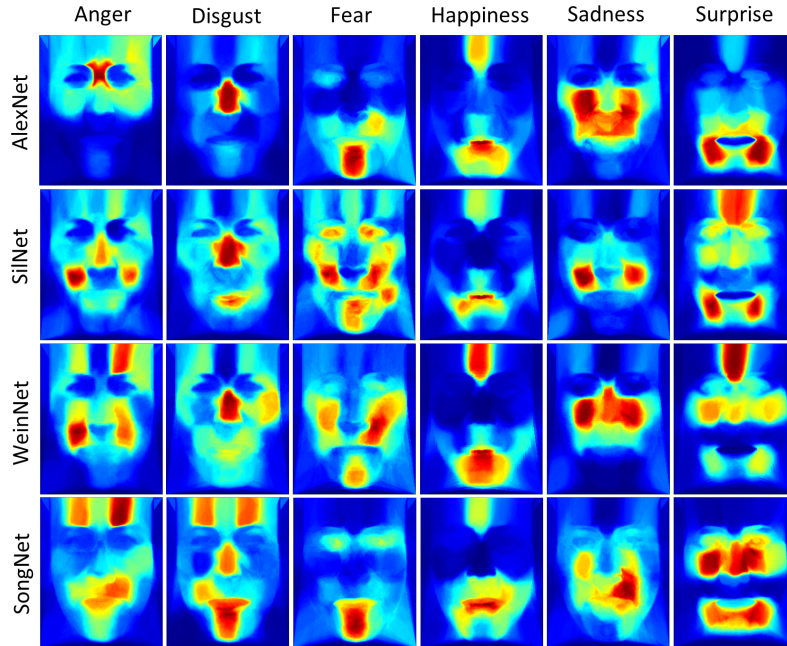


Fig. 8: Resulting heatmaps of the four networks not using pre-trained weights. By columns, heatmaps of the same network for the different expressions. By rows, heatmaps of the different networks for the same expression.

Figures 8 and 9 display the heatmaps for a specific network and facial expression. The first one displays only networks not using pre-trained weights (i.e. SilNet, WeiNet, AlexNet and SongNet), while the second one displays the networks using pre-trained weights on ImageNet (i.e. VGG16, VGG19, ResNet50, ResNet101V2, InceptionV3, Xception, MobileNetV3, and EfficientNetV2). At first glance, it seems that the heatmaps in Figure 8 have more scattered hot regions than Figure 9, and that there is more similarity between heatmaps of models with pre-trained weights than with models without a pre-training, which is later explored in depth in subsection 5.4.

A specially important region for the pre-trained networks appears to be the mouth, which is highlighted in almost all 48 heatmaps shown in Figure 9. The eyes are also of special importance in the recognition of fear and surprise for all networks. The nose, on the other hand, seems important for the anger, disgust and sadness expressions, although not for all networks. In the case of VGG16 and VGG19, the heatmaps are pretty alike for all expressions.

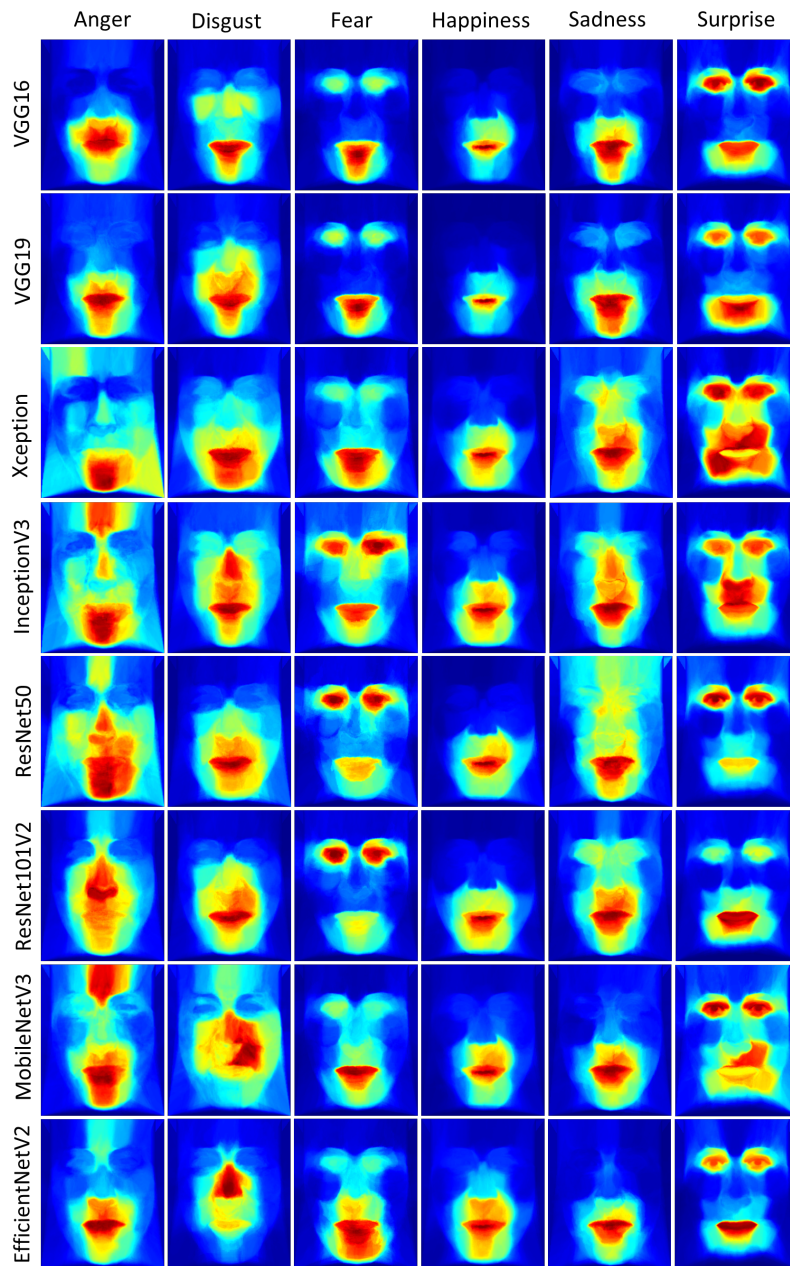


Fig. 9: Resulting heatmaps of the eight networks using pre-trained weights. By columns, heatmaps of the same network for the different expressions. By rows, heatmaps of the different networks for the same expression.

5.3 Difference between network heatmaps and Ekman masks

The IoU results between the Ekman masks and the thresholded heatmaps of the different networks, for each expression, are shown in Table 3.

Table 3: IoU between the computed heatmaps for each network and expression and the Ekman masks. Last column shows the average between expressions, for each network. Last row shows the average between networks, for each expression. The best result for each column is highlighted in bold.

	Anger	Disgust	Fear	Happiness	Sadness	Surprise	Avg.
SilNet	0.2565	0.4336	0.3845	0.115	0.2902	0.2908	0.2951
WeiNet	0.2148	0.3352	0.2549	0.1011	0.2996	0.1581	0.2273
AlexNet	0.3311	0.1873	0.1259	0.091	0.3175	0.1869	0.2066
SongNet	0.352	0.2338	0.0864	0.2636	0.2943	0.1632	0.2322
InceptionV3	0.3073	0.6412	0.2444	0.2261	0.2755	0.2513	0.3243
VGG19	0.124	0.632	0.1294	0.1727	0.1109	0.305	0.2457
VGG16	0.1164	0.5752	0.1273	0.1523	0.1171	0.2936	0.2303
ResNet50	0.1944	0.5156	0.2226	0.2797	0.4236	0.3252	0.3269
ResNet101V2	0.1811	0.5697	0.2004	0.2793	0.3446	0.3152	0.315
Xception	0.1545	0.4139	0.2026	0.2315	0.2732	0.251	0.2544
MobileNetV3	0.3322	0.5250	0.2594	0.1849	0.1039	0.2555	0.2768
EfficientNetV2	0.2401	0.7212	0.2069	0.2583	0.0990	0.3242	0.3083
Avg.	0.2337	0.4820	0.2037	0.1963	0.2458	0.2600	0.2702

Out of all the trained networks, the one with the best performance, averaging all facial expressions, is ResNet50 with a value of approximately 0.33, followed closely by InceptionV3, ResNet101V2 and EfficientNetV2. On the other hand, averaging by networks, we can observe that the "Disgust" facial expression gets the most similar heatmaps to the Ekman mask, with a mean value of approximately 0.48, with a difference of almost two tenths higher than the rest. In fact, EfficientNetV2 gets up to a score of 0.72 for this expression, the highest value among all networks and expressions.

Since the average IoU between the networks' heatmaps and the Ekman masks is pretty low for all networks (lower than 0.33 IoU), the results seem to point out a significant difference in the relevant regions when classifying the facial expressions, between the trained networks and the constructed Ekman masks.

5.4 Similarity between heatmaps

Figure 10 shows the dendograms constructed using the normalized correlation coefficient to assess the difference between heatmaps for a network and an expression. As already seen in Figures 8 and 9, there appear two main clusters for the majority of the expressions: models with pre-training and models with no pre-training. This seems to indicate that the pre-training on ImageNet used by VGG16, VGG19, ResNet50, ResNet101V2, InceptionV3, Xception, MobileNetV3, and EfficientNetV2 leads them

to converge to similar solutions for the facial expression classification problem. In addition, the difference between heatmaps for this cluster tends to be smaller than that between heatmaps of the cluster of models not using pre-trained weights (i.e. SilNet, WeiNet, AlexNet and SongNet): 0.2 vs. 0.35 in disgust, 0.05 vs. 0.2 in happiness, 0.15 vs. 0.25 in sadness, and 0.2 vs. 0.5 in surprise respectively.

A high similarity between some of the networks can also be observed. For example, SilNet and WeiNet’s heatmaps are very close for the majority of the facial expressions, which is also the case of VGG16 and VGG19.

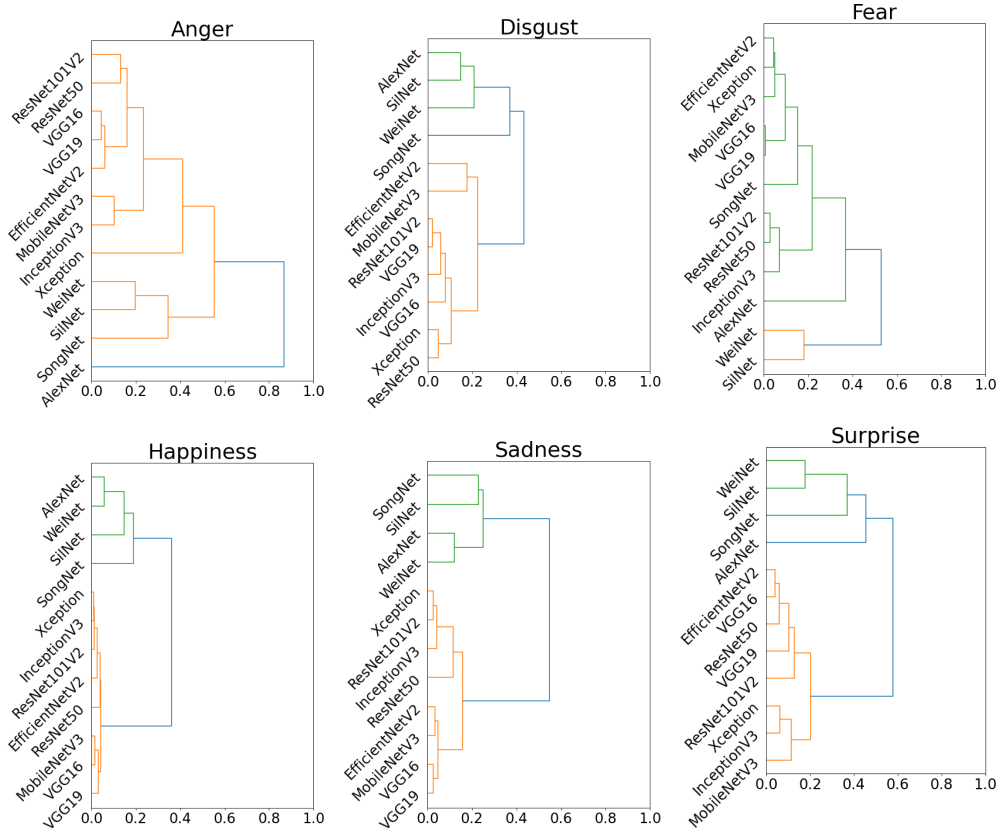


Fig. 10: Dendrograms grouping the heatmaps of the different networks by facial expression, using the normalized correlation coefficient.

6 Discussion

Regarding the accuracy, results showed consistently high accuracy across all tested CNNs, ranging from 80% to 84%, with the exception of ResNet50 (74%). We selected a broad number of networks introduced to the community between 2012 and 2022, varying in pre-training, architecture, parameters, and the purpose of design, as three

of them were specifically built for facial expression recognition. As already commented, improving the performance was out of the scope of this work, but the results show that despite the diversity in design, complexity and depth, all networks demonstrated comparable accuracy levels, even ResNet50, allowing the next studies.

Regarding the important regions used by the networks for classification, we compared qualitatively the heatmaps. Taking all networks in global (see 7), we find expressions that observe similar zones as humans, others that consider a subset of the important regions, and others that included regions not considered by human perception considering Ekman’s descriptions [69]. The happiness expression presents a human-like behaviour, focusing on the lower part of the face, probably observing the smile. The expression of disgust also highlights important regions for humans such as the nose and mouth, however, the brows-forehead section is less noticeable. A third case are expressions like anger, although a notable region is the lower face part, the network is considering many other face regions not related to AUs. When analyzing the heatmaps between pre-trained networks and non-pre-trained (see 8 and 9), the former focuses on more localized regions, while the latter considers more dispersed regions within the face. This qualitative observation is consistent with the computed dendograms, where non-pre-trained networks cluster together in four expressions out of six (disgust, happiness, surprise and sadness). Similar groupings happen for those CNNs that share a common base architecture (e.g. SilNet and WeiNet or VGG16 and VGG19). This is most probably due to their alike architecture, which makes them learn in a similar way.

Finally, regardless of the CNN’s architecture, the study findings indicate that the CNNs did not resemble Ekman’s masks based on the AUs. These findings can relate with two challenges in the community. On the one hand, the computer vision community aims at developing models with better performance, making the networks smaller or training them with less data [70]. In this sense, integrating principles of human learning can help the AI reduce data requirement and increase its performance, reliability and robustness as shown in [71–73]. On the other hand, users expect AI to be (i) accurate, (ii) trustworthy and responsible [74]. Endeavors have traditionally been done to improve the accuracy of automated facial expressions recognition, and research on responsible AI applied to FER is still scarce. To achieve trustworthy AI, a strategy is to explain to users how the AI reached a specific outcome to understand the rationale behind the AI functioning. Aligning the human visual system with the CNNs working may make the model more human-understandable [75]. This aligns with the cognitive anthropomorphism of humans, that is, the tendency to attribute human-like qualities to non-human entities or objects. Therefore, when the rationale makes sense to the user, it can help building trust towards AI, which can be considered as “the extent to which a user is confident in, and willing to act on the basis of, the recommendations, actions, and decisions of an artificially intelligent decision aid” [76].

7 Conclusion

In this paper, we studied the correspondence between human and automatic facial expression recognition. To do so, we trained twelve different networks for this task, and

then applied an explanation and standardization process to unveil the most important face regions for the recognition of each expression, for each network. We then evaluated qualitatively the obtained results, compared the performance of the different networks and computed the similarity with Ekman masks, constructed based on the AUs involved in the recognition of every expression.

The results show a big variability in which regions can be important for a model's classification of the facial expressions, especially for models not using pre-trained weights. The use of pre-trained weights showed a big impact in the obtained heatmaps, bringing them closer in the selection of important facial regions. In spite of this, none of the networks achieved an average similarity above 33% IoU with the computed Ekman masks, which demonstrates a poor correspondence between what the AI models and humans consider important in facial expressions recognition.

One of the limitations of the study is that we have focused on CNNs, therefore, future work could explore other types of models. We should also determine whether this similarity between humans and AI in FER is deemed necessary to achieve the trust of the users, or explore the suitability of improving and adapting the AI models or training datasets to meet the humans expectations while not decreasing the performance.

8 Acknowledgments

This work has been supported by Grant PID2019-104829RA-I00 funded by MCIN/AEI /10.13039/501100011033, EXPLainable Artificial INtelligence systems for health and well-beING (EXPLAINING).

In addition, F.X. Gayà-Morey also acknowledges the importance of the FPU scholarship from the Ministry of European Funds, University and Culture of the Government of the Balearic Islands.

References

- [1] Barrett, L.F., Adolphs, R., Marsella, S., Martinez, A.M., Pollak, S.D.: Emotional Expressions Reconsidered: Challenges to Inferring Emotion From Human Facial Movements. *Psychological Science in the Public Interest* **20**(1), 1–68 (2019) <https://doi.org/10.1177/1529100619832930>
- [2] Ekman, P.: An argument for basic emotions. *Cognition and Emotion* **6**(3-4), 169–200 (1992) <https://doi.org/10.1080/02699939208411068>
- [3] Grabowski, K., Rynkiewicz, A., Lassalle, A., Baron-Cohen, S., Schuller, B., Cummins, N., Baird, A., Podgórska-Bednarz, J., Pieniążek, A., Łucka, I.: Emotional expression in psychiatric conditions: New technology for clinicians. *Psychiatry and Clinical Neurosciences* **73**(2), 50–62 (2019) <https://doi.org/10.1111/pcn.12799>
- [4] Barreto, A.M.: Application of facial expression studies on the field of marketing. *Emotional expression: the brain and the face* **9**(June), 163–189 (2017)

- [5] Shen, J., Yang, H., Li, J., Cheng, Z.: Assessing learning engagement based on facial expression recognition in MOOC’s scenario. *Multimedia Systems* **28**(2), 469–478 (2022) <https://doi.org/10.1007/s00530-021-00854-x>
- [6] Medjden, S., Ahmed, N., Lataifeh, M.: Adaptive user interface design and analysis using emotion recognition through facial expressions and body posture from an RGB-D sensor. *PLoS ONE* **15**(7), 0235908 (2020) <https://doi.org/10.1371/journal.pone.0235908>
- [7] Ramis, S., Buades, J.M., Perales, F.J.: Using a Social Robot to Evaluate Facial Expressions in the Wild. *Sensors* **20**(23) (2020) <https://doi.org/10.3390/s20236716>
- [8] Pantic, M., Rothkrantz, L.J.M.: Automatic analysis of facial expressions: the state of the art. *IEEE Transactions on Pattern Analysis and Machine Intelligence* **22**(12), 1424–1445 (2000) <https://doi.org/10.1109/34.895976>
- [9] Fasel, B., Luetttin, J.: Automatic facial expression analysis: a survey. *Pattern Recognition* **36**(1), 259–275 (2003) [https://doi.org/10.1016/S0031-3203\(02\)00052-3](https://doi.org/10.1016/S0031-3203(02)00052-3)
- [10] Li, S., Deng, W.: Deep Facial Expression Recognition: A Survey. *IEEE Transactions on Affective Computing*, 1 (2020) <https://doi.org/10.1109/TAFFC.2020.2981446>
- [11] Mellouk, W., Handouzi, W.: Facial emotion recognition using deep learning: review and insights. *Procedia Computer Science* **175**, 689–694 (2020) <https://doi.org/10.1016/j.procs.2020.07.101> . The 17th International Conference on Mobile Systems and Pervasive Computing (MobiSPC),The 15th International Conference on Future Networks and Communications (FNC),The 10th International Conference on Sustainable Energy Information Technology
- [12] Mueller, S.T.: Cognitive anthropomorphism of ai: How humans and computers classify images. *Ergonomics in Design* **28**(3), 12–19 (2020) <https://doi.org/10.1177/1064804620920870>
- [13] Borowski, J., Funke, C.M., Stosio, K., Brendel, W., Wallis, T.S.A., Bethge, M.: The Notorious Difficulty of Comparing Human and Machine Perception, 642–646 (2019) <https://doi.org/10.32470/ccn.2019.1295-0>
- [14] Geirhos, R., Janssen, D.H.J., Schütt, H.H., Rauber, J., Bethge, M., Wichmann, F.A.: Comparing deep neural networks against humans: object recognition when the signal gets weaker (2017)
- [15] Kheradpisheh, S.R., Ghodrati, M., Ganjtabesh, M., Masquelier, T.: Deep Networks Can Resemble Human Feed-forward Vision in Invariant Object Recognition. *Scientific Reports* **6**(1), 32672 (2016) <https://doi.org/10.1038/srep32672>

- [16] Jacob, G., Pramod, R.T., Katti, H., Arun, S.P.: Qualitative similarities and differences in visual object representations between brains and deep networks. *Nature Communications* **12**(1), 1872 (2021) <https://doi.org/10.1038/s41467-021-22078-3>
- [17] Ullman, S., Assif, L., Fetaya, E., Harari, D.: Atoms of recognition in human and computer vision. *Proceedings of the National Academy of Sciences* **113**(10), 2744–2749 (2016) <https://doi.org/10.1073/pnas.1513198113>
- [18] Ekman, P., Friesen, W.V.: *Manual for the Facial Action Coding System*. Consulting Psychologists Press, ??? (1978)
- [19] Khan, R.A., Meyer, A., Konik, H., Bouakaz, S., Khan, R.A., Meyer, A., Konik, H., Bouakaz, S.: Human vision inspired framework for facial expressions recognition. In: *Image Processing (ICIP), 2012 19th IEEE International Conference On*, Sep 2012, Orlando, FL, United States., pp. 2593–2596 (2013)
- [20] Benitez-Quiroz, C.F., Wang, Y., Martinez, A.M.: Recognition of Action Units in the Wild with Deep Nets and a New Global-Local Loss. In: *2017 IEEE International Conference on Computer Vision (ICCV)*, pp. 3990–3999 (2017). <https://doi.org/10.1109/ICCV.2017.428>
- [21] Pham, T.T.D., Won, C.S.: Facial action units for training convolutional neural networks. *IEEE Access* **7**, 77816–77824 (2019) <https://doi.org/10.1109/ACCESS.2019.2921241>
- [22] Benitez-Quiroz, C.F., Srinivasan, R., Feng, Q., Wang, Y., Martinez, A.M.: *EmotioNet Challenge: Recognition of facial expressions of emotion in the wild* (2017)
- [23] Barredo Arrieta, A., Díaz-Rodríguez, N., Del Ser, J., Bennetot, A., Tabik, S., Barbado, A., Garcia, S., Gil-Lopez, S., Molina, D., Benjamins, R., Chatila, R., Herrera, F.: Explainable Artificial Intelligence (XAI): Concepts, taxonomies, opportunities and challenges toward responsible AI. *Information Fusion* **58**, 82–115 (2020) <https://doi.org/10.1016/j.inffus.2019.12.012> [arXiv:1910.10045](https://arxiv.org/abs/1910.10045)
- [24] Adadi, A., Berrada, M.: Peeking inside the black-box: A survey on explainable artificial intelligence (xai). *IEEE Access* **6**, 52138–52160 (2018) <https://doi.org/10.1109/ACCESS.2018.2870052>
- [25] Gunning, D., Aha, D.W.: DARPA’s Explainable Artificial Intelligence (XAI) Program. *AI Mag.* **40**(2), 44–58 (2019) <https://doi.org/10.1609/aimag.v40i2.2850>
- [26] Kandeel, A.A., Abbas, H.M., Hassanein, H.S.: Explainable Model Selection of a Convolutional Neural Network for Driver’s Facial Emotion Identification. In: *Del Bimbo, A., Cucchiara, R., Sclaroff, S., Farinella, G.M., Mei, T., Bertini,*

- M., Escalante, H.J., Vezzani, R. (eds.) Pattern Recognition. ICPR International Workshops and Challenges, pp. 699–713. Springer, Cham (2021)
- [27] Weitz, K., Hassan, T., Schmid, U., Garbas, J.: Deep-learned faces of pain and emotions: Elucidating the differences of facial expressions with the help of explainable AI methods. *tm - Technisches Messen* **86**, 404–412 (2019)
- [28] Manresa-Yee, C., Ramis, S., Buades, J.M.: Analysis of Gender Differences in Facial Expression Recognition Based on Deep Learning Using Explainable Artificial Intelligence. *International Journal of Interactive Multimedia and Artificial Intelligence* (In press) <https://doi.org/10.9781/ijimai.2023.04.003>
- [29] Manresa-Yee, C., Ramis Guarinos, S., Buades Rubio, J.M.: Facial expression recognition: Impact of gender on fairness and expressions. In: Proceedings of the XXII International Conference on Human Computer Interaction. Interacción '22. Association for Computing Machinery, New York, NY, USA (2022). <https://doi.org/10.1145/3549865.3549904>
- [30] Schiller, D., Huber, T., Dietz, M., André, E.: Relevance-Based Data Masking: A Model-Agnostic Transfer Learning Approach for Facial Expression Recognition. *Frontiers in Computer Science* **2**, 6 (2020) <https://doi.org/10.3389/fcomp.2020.00006>
- [31] Heimerl, A., Weitz, K., Baur, T., Andre, E.: Unraveling ML Models of Emotion with NOVA: Multi-Level Explainable AI for Non-Experts. *IEEE Transactions on Affective Computing* **1**(1), 1–13 (2020) <https://doi.org/10.1109/TAFFC.2020.3043603>
- [32] Khorrami, P., Paine, T.L., Huang, T.S.: Do Deep Neural Networks Learn Facial Action Units When Doing Expression Recognition? In: 2015 IEEE International Conference on Computer Vision Workshop (ICCVW), pp. 19–27 (2015). <https://doi.org/10.1109/ICCVW.2015.12>
- [33] Lucey, P., Cohn, J.F., Kanade, T., Saragih, J., Ambadar, Z., Matthews, I.: The extended cohn-kanade dataset (ck+): A complete dataset for action unit and emotion-specified expression. In: 2010 Ieee Computer Society Conference on Computer Vision and Pattern Recognition-workshops, pp. 94–101 (2010). IEEE
- [34] Susskind, J.M., Anderson, A.K., Hinton, G.E.: The Toronto Face Database. Technical report
- [35] Prajod, P., Schiller, D., Huber, T., André, E.: In: Shaban-Nejad, A., Michalowski, M., Bianco, S. (eds.) Do Deep Neural Networks Forget Facial Action Units?—Exploring the Effects of Transfer Learning in Health Related Facial Expression Recognition, pp. 217–233. Springer, Cham (2022). https://doi.org/10.1007/978-3-030-93080-6_16

- [36] Lucey, P., Cohn, J.F., Prkachin, K.M., Solomon, P.E., Matthews, I.: Painful data: The unbc-mcmaster shoulder pain expression archive database. In: 2011 IEEE International Conference on Automatic Face & Gesture Recognition (FG), pp. 57–64 (2011). <https://doi.org/10.1109/FG.2011.5771462>
- [37] Deramgozin, M., Jovanovic, S., Rabah, H., Ramzan, N.: A Hybrid Explainable AI Framework Applied to Global and Local Facial Expression Recognition, (2021). <https://doi.org/10.1109/IST50367.2021.9651357>
- [38] Gund, M., Bharadwaj, A.R., Nwogu, I.: Interpretable emotion classification using temporal convolutional models. In: 2020 25th International Conference on Pattern Recognition (ICPR), pp. 6367–6374 (2021). <https://doi.org/10.1109/ICPR48806.2021.9412134>
- [39] Davison, A.K., Lansley, C., Costen, N., Tan, K., Yap, M.H.: Samm: A spontaneous micro-facial movement dataset. *IEEE Transactions on Affective Computing* **9**(1), 116–129 (2018) <https://doi.org/10.1109/TAFFC.2016.2573832>
- [40] Zhou, L., Yang, A., Meng, M., Zhou, K.: Emerged human-like facial expression representation in a deep convolutional neural network. *Science Advances* **8**(12), 4383 (2022) <https://doi.org/10.1126/sciadv.abj4383>
- [41] Yin, L., Wei, X., Sun, Y., Wang, J., Rosato, M.J.: A 3d facial expression database for facial behavior research. In: 7th International Conference on Automatic Face and Gesture Recognition (FGR06), pp. 211–216 (2006). IEEE
- [42] Lyons, M.J., Akamatsu, S., Kamachi, M., Gyoba, J., Budynek, J.: The japanese female facial expression (jaffe) database. In: Third International Conference on Automatic Face and Gesture Recognition, pp. 14–16 (1998)
- [43] Olszanowski, M., Pochwatko, G., Kuklinski, K., Scibor-Rylski, M., Lewinski, P., Ohme, R.K.: Warsaw set of emotional facial expression pictures: a validation study of facial display photographs. *Frontiers in psychology* **5**, 1516 (2015)
- [44] Ramis, S., Buades, J.M., Perales, F.J., Manresa-Yee, C.: A novel approach to cross dataset studies in facial expression recognition. *Multimedia Tools Appl.* **81**(27), 39507–39544 (2022) <https://doi.org/10.1007/s11042-022-13117-2>
- [45] Lisani, J.-L., Ramis, S., Perales, F.J.: A contrario detection of faces: A case example. *SIAM Journal on Imaging Sciences* **10**(4), 2091–2118 (2017) <https://doi.org/10.1137/17M1118774>
- [46] Kazemi, V., Sullivan, J.: One millisecond face alignment with an ensemble of regression trees. In: 2014 IEEE Conference on Computer Vision and Pattern Recognition, pp. 1867–1874 (2014). <https://doi.org/10.1109/CVPR.2014.241>
- [47] Wu, Y., Ji, Q.: Facial Landmark Detection: A Literature Survey. *International*

- [48] McReynolds, T., Blythe, D.: Chapter 3 - color, shading, and lighting. In: McReynolds, T., Blythe, D. (eds.) *Advanced Graphics Programming Using OpenGL*. The Morgan Kaufmann Series in Computer Graphics, pp. 35–56. Morgan Kaufmann, San Francisco (2005). <https://doi.org/10.1016/B978-155860659-3.50005-6>
- [49] Krizhevsky, A., Sutskever, I., Hinton, G.E.: Imagenet classification with deep convolutional neural networks. In: Pereira, F., Burges, C.J., Bottou, L., Weinberger, K.Q. (eds.) *Advances in Neural Information Processing Systems*, vol. 25. Curran Associates, Inc., ??? (2012)
- [50] Simonyan, K., Zisserman, A.: *Very Deep Convolutional Networks for Large-Scale Image Recognition* (2015)
- [51] He, K., Zhang, X., Ren, S., Sun, J.: *Deep Residual Learning for Image Recognition* (2015)
- [52] Szegedy, C., Vanhoucke, V., Ioffe, S., Shlens, J., Wojna, Z.: *Rethinking the Inception Architecture for Computer Vision* (2015)
- [53] Chollet, F.: *Xception: Deep learning with depthwise separable convolutions*. In: *Proceedings of the IEEE Conference on Computer Vision and Pattern Recognition (CVPR)* (2017)
- [54] Howard, A., Sandler, M., Chu, G., Chen, L.-C., Chen, B., Tan, M., Wang, W., Zhu, Y., Pang, R., Vasudevan, V., Le, Q.V., Adam, H.: *Searching for MobileNetV3* (2019)
- [55] Tan, M., Le, Q.V.: *EfficientNetV2: Smaller Models and Faster Training* (2021)
- [56] Song, I., Kim, H.-J., Jeon, P.B.: *Deep learning for real-time robust facial expression recognition on a smartphone*. In: *2014 IEEE International Conference on Consumer Electronics (ICCE)*, pp. 564–567 (2014). <https://doi.org/10.1109/ICCE.2014.6776135>
- [57] Li, W., Li, M., Su, Z., Zhu, Z.: *A deep-learning approach to facial expression recognition with candid images*. In: *2015 14th IAPR International Conference on Machine Vision Applications (MVA)*, pp. 279–282 (2015). IEEE
- [58] He, K., Zhang, X., Ren, S., Sun, J.: *Deep residual learning for image recognition*. In: *2016 IEEE Conference on Computer Vision and Pattern Recognition (CVPR)*, pp. 770–778 (2016). <https://doi.org/10.1109/CVPR.2016.90>
- [59] Szegedy, C., Liu, W., Jia, Y., Sermanet, P., Reed, S., Anguelov, D., Erhan, D.,

- Vanhoucke, V., Rabinovich, A.: Going Deeper with Convolutions (2014)
- [60] Howard, A.G., Zhu, M., Chen, B., Kalenichenko, D., Wang, W., Weyand, T., Andreetto, M., Adam, H.: MobileNets: Efficient Convolutional Neural Networks for Mobile Vision Applications (2017)
- [61] Tan, M., Le, Q.V.: EfficientNet: Rethinking Model Scaling for Convolutional Neural Networks (2020)
- [62] Ribeiro, M.T., Singh, S., Guestrin, C.: "Why should i trust you?" Explaining the predictions of any classifier. Proceedings of the ACM SIGKDD International Conference on Knowledge Discovery and Data Mining **13-17-Aug**, 1135–1144 (2016) <https://doi.org/10.1145/2939672.2939778>
- [63] van der Velden, B.H.M., Kuijf, H.J., Gilhuijs, K.G.A., Viergever, M.A.: Explainable artificial intelligence (xai) in deep learning-based medical image analysis. Medical Image Analysis **79**, 102470 (2022) <https://doi.org/10.1016/j.media.2022.102470>
- [64] Alicioglu, G., Sun, B.: A survey of visual analytics for explainable artificial intelligence methods. Computers & Graphics **102**, 502–520 (2022) <https://doi.org/10.1016/j.cag.2021.09.002>
- [65] Achanta, R., Shaji, A., Smith, K., Lucchi, A., Fua, P., Süsstrunk, S.: Slic superpixels compared to state-of-the-art superpixel methods. IEEE Transactions on Pattern Analysis and Machine Intelligence **34**(11), 2274–2282 (2012) <https://doi.org/10.1109/TPAMI.2012.120>
- [66] Friesen, W.V., Ekman, P.: EMFACS-7: Emotional Facial Action Coding System. (1983)
- [67] Perveen, N., Mohan, C.: Configural Representation of Facial Action Units for Spontaneous Facial Expression Recognition in the Wild. In: 15th International Conference on Computer Vision Theory and Applications (2020). <https://doi.org/10.5220/0009099700930102>
- [68] Otsu, N.: A threshold selection method from gray-level histograms. IEEE Transactions on Systems, Man, and Cybernetics **9**(1), 62–66 (1979) <https://doi.org/10.1109/TSMC.1979.4310076>
- [69] Ekman, P.: Universals and cultural differences in facial expressions of emotion. Nebraska Symposium on Motivation **19**, 207–283 (1971)
- [70] Lindsay, G.W.: Convolutional neural networks as a model of the visual system: Past, present, and future. Journal of Cognitive Neuroscience **33**(10), 2017–2031 (2021) <https://doi.org/10.1162/jocn.a.01544> arXiv:2001.07092

- [71] Deng, C., Ji, X., Rainey, C., Zhang, J., Lu, W.: Integrating machine learning with human knowledge. *iScience* **23**(11), 101656 (2020) <https://doi.org/10.1016/j.isci.2020.101656>
- [72] Boyd, A., Tinsley, P., Bowyer, K., Czajka, A.: CYBORG: Blending Human Saliency Into the Loss Improves Deep Learning (2022)
- [73] Schiller, D., Huber, T., Dietz, M., André, E.: Relevance-Based Data Masking: A Model-Agnostic Transfer Learning Approach for Facial Expression Recognition. *Frontiers in Computer Science* **2**, 6 (2020) <https://doi.org/10.3389/fcomp.2020.00006>
- [74] Watson, D.: The Rhetoric and Reality of Anthropomorphism in Artificial Intelligence. *Minds and Machines* **29**(3), 417–440 (2019) <https://doi.org/10.1007/s11023-019-09506-6>
- [75] Guidotti, R., Monreale, A., Ruggieri, S., Turini, F., Pedreschi, D., Giannotti, F.: A Survey Of Methods For Explaining Black Box Models (2018)
- [76] Madsen, M., Gregor, S.D.: Measuring human-computer trust. In: Proceedings of 11th Australasian Conference on Information Systems (2000)